

D. I. Trubetskov, E. S. Mchedlova, V. G. Anfinogentov, V. I. Ponomarenko,
and N. M. Ryskin

Saratov State University, College of Applied Science, Saratov 410026, Russia

(Received 26 February 1996; accepted for publication 9 July 1996)

We discuss some problems, concerning the application of nonlinear dynamics methods and ideas to vacuum microwave electronics. We consider such phenomena as solitons, deterministic chaos and pattern formation in different models of electron flows and devices. Our results reveal that microwave electronics is an interesting field of application of nonlinear dynamics. © 1996 American Institute of Physics. [S1054-1500(96)01903-9]

Applications of nonlinear science to real systems are continually being developed, and in this work such applications to vacuum microwave electronic devices are explored. Nonlinear waves in electron beam are considered and processes of solitary waves formation and interaction are studied. One of the simplest electron systems demonstrating chaotic behaviour, called the Pierce diode, is investigated and a simple description in a form of coupled piecewise maps is suggested. Experimental and numerical simulations of a new microelectronic oscillator based on a field emission triode also exhibit bifurcations along the transition to deterministic chaos. Finally, a phenomenological model of electron turbulence consisting of a chain of coupled small volumes with electron oscillators is discussed.

I. INTRODUCTION

The present paper deals with the microwave (MW) electron devices which are typical examples of distributed nonlinear systems. Such systems are among the most significant subjects of nonlinear dynamics. Here we speak mostly about nonrelativistic devices where the electron beam velocity is much lower than the velocity of light in vacuum. The main purpose of this work is to show the ways of using ideas and methods of nonlinear dynamics in MW electronics. The paper summarizes the most important results of the research carried out during the last five years at Saratov State University.

The article is organized as follows. In the section II we consider nonlinear waves in electron beams. Solitary wave solutions are obtained analytically. The processes of their formation and interaction are simulated numerically. The section III deals with one of the simplest electron systems, demonstrating complex behaviour including deterministic chaos. This system, called the Pierce diode, is investigated by the numerical simulation. A simple model in the form of coupled piecewise maps is suggested, which gives a proper description of chaotic oscillations in the system. In the section IV a new type of vacuum microelectronic oscillator based on a field-emission triode is studied numerically and experimentally. Deterministic chaos is observed and some universal features of the bifurcation scenario are found. In section V a phenomenological model of electron turbulence is proposed, which consists of a chain of coupled small vol-

umes containing electron oscillators. Regimes of spatio-temporal chaos are observed.

II. NONLINEAR WAVES IN ELECTRON BEAMS

The Russian poet Vladimir Vysotskii once wrote in one of his poems about water waves:

The stormy night;
And while the sand is coming all apart
Hereafter being patched up with the snow-white foam,
I'm looking down on those poor waves
And watch them having their stubborn heads all broken.

It is precisely these "heads broken" that made the MW electronics specialists abandon the fluid model of electron beam in favour of the "large particles" method.

It is essential to recall that the linear theory of different types of MW electron devices usually employs the concept of interaction of electromagnetic waves with various types of linear waves in electron beams, such as space-charge waves, cyclotronic, synchronic waves, etc. (see, e.g., Ref. 1). But the nonlinear theory of such devices is always based on the numerical simulation with the "large particles" method which gives the opportunity of a proper description of overtaking of some electrons by others.² Recall that overtaking corresponds to wave breaking. Quite naturally there arose a question if there were nonlinear analogies to the waves mentioned before.

The "soliton boom" in the last two decades gave rise to papers in which equations describing this or that MW device came down to one of the standard equations of nonlinear wave theory, possessing soliton solutions, mostly the nonlinear Schrödinger equation or the Korteweg – de Vries (KdV) equation (see the review in Ref. 3). It is obvious that such an approach always leaves open the question of the limits of the application. In our works^{4,5} we have performed analytical and numerical investigations of solitary waves based on the fluid model of electron flow.

Let us consider a cylindrical charge-neutralized electron beam of radius r moving in an infinitely strong longitudinal magnetic field along the axis of a drift tube with perfectly conducting walls. The tube axis coincides with the x -axis. If velocity perturbations are too low to cause electron overtaking, the system can be described by the following hydrodynamic equations:

$$\frac{\partial v}{\partial t} + v \frac{\partial v}{\partial x} = \frac{\partial \varphi}{\partial x}, \quad (1)$$

$$\frac{\partial \rho}{\partial t} + \frac{\partial(\rho v)}{\partial x} = 0. \quad (2)$$

The variables in equations (1) and (2) are dimensionless and normalized in the following way: velocity v and space-charge density ρ are referred to nondisturbed values v_0 and ρ_0 , space-charge field potential φ to mv_0^2/e , time to ω_p^{-1} and coordinate to v_0/ω_p , where $\omega_p = (e\rho_0/m\varepsilon_0)^{1/2}$ is the plasma frequency.

For the potential φ we use the well-known relation²

$$\varphi(x) = \frac{1}{2k_\perp} \int_{-\infty}^{\infty} (\rho(x') - 1) \exp[-k_\perp |x - x'|] dx', \quad (3)$$

where $k_\perp = \alpha/r$ ($1 \leq \alpha \leq 2$). We can rewrite equation (3), for convenience, in the differential form

$$\frac{\partial^2 \varphi}{\partial x^2} - k_\perp^2 \varphi = \rho - 1. \quad (4)$$

To find the analytical solution of equations (1), (2), and (4) it is necessary to search for stationary waves that are solutions dependent on $\vartheta = x - ut$, where $u = \text{const}$ is the wave velocity. Integrating equations (1) and (2) with the boundary conditions

$$v = 1, \quad \rho = 1, \quad \varphi = 0 \quad \text{at} \quad \vartheta \rightarrow \pm \infty \quad (5)$$

and substituting the result in (4) we get the "nonlinear oscillator" equation

$$\frac{d^2 \varphi}{d\vartheta^2} = k_\perp^2 \varphi + [1 + 2\varphi/(1-u)^2]^{-1/2} - 1. \quad (6)$$

The potential energy of such an oscillator can be described by the function [we should note, that if $|2\varphi/(1-u)^2| \ll 1$ (weak nonlinearity), then expanding the right-hand sides of relations (6) and (7) a series up to second-order terms we could obtain the equations having solutions in the form of KdV solitons⁶]

$$W(\varphi) = \varphi - \frac{k_\perp^2 \varphi^2}{2} + (1-u)^2 \left[1 - \sqrt{1 + \frac{2\varphi}{(1-u)^2}} \right], \quad (7)$$

which has two extreme points at $\varphi = 0$ and $\varphi = \varphi^*$,

$$\varphi^* = \frac{4-M^2}{4k_\perp^2} - \frac{1}{2k_\perp^2} \sqrt{\frac{M^4}{4} + 2M^2}, \quad (8)$$

where $M = k_\perp |1-u|$ and has the meaning of a Mach number.

When $M < 1$, the equilibrium state at $\varphi = 0$ is stable, but at $\varphi = \varphi^* > 0$ it is unstable. When $M > 1$ the equilibrium state at $\varphi = 0$ is unstable, and at $\varphi^* < 0$ we get a stable one. Hence, in both cases the solitary wave solution is possible. But for $M < 1$ the solutions obtained do not satisfy the boundary conditions (5). Thus in this case only periodic solutions are to be expected. We are interested in solitary waves and thus we assume that the condition $M > 1$ is satisfied. The analysis shows that the solitary wave is stable for $M < 2$, so M has to satisfy the inequality $1 < M < 2$. Thus it follows from the definition of M , that velocity u is subject to the inequality

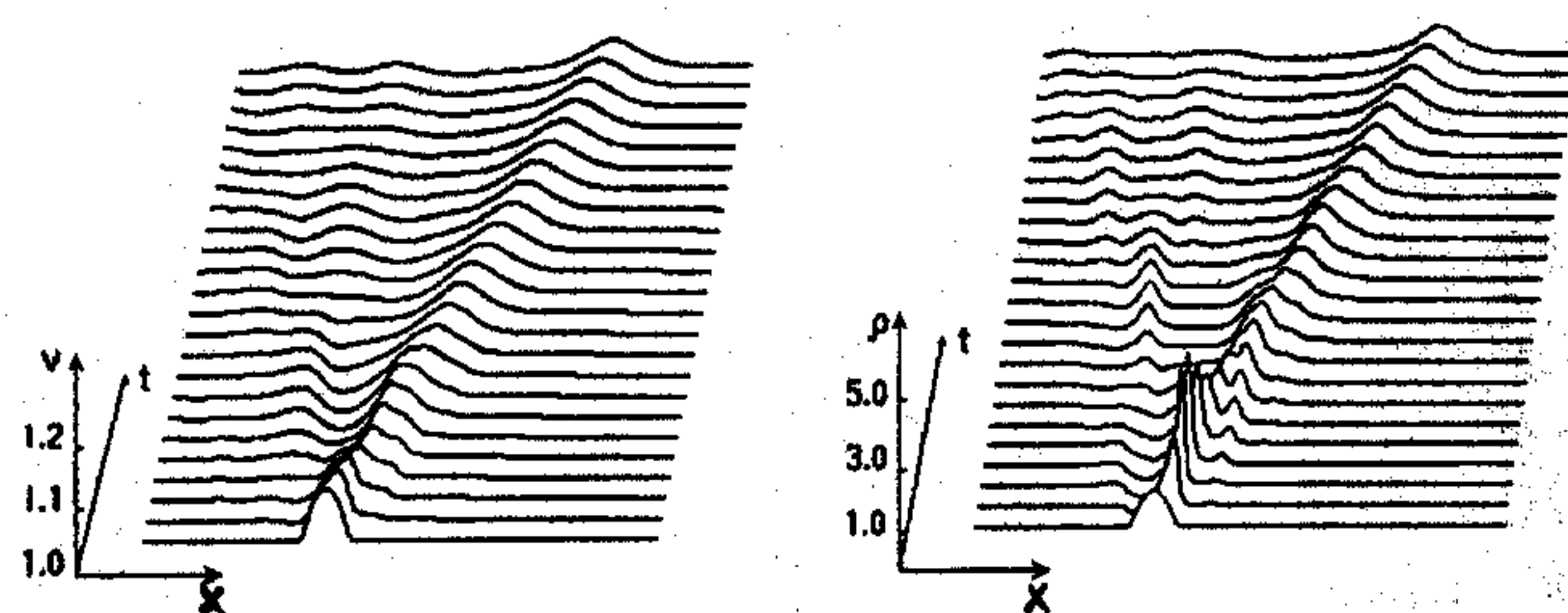


FIG. 1. Formation of fast space-charge solitary wave.

$$1 + 1/k_\perp < u < 1 + 2/k_\perp \quad (9)$$

for a fast solitary wave and

$$1 - 2/k_\perp < u < 1 - 1/k_\perp \quad (10)$$

for a slow wave. Note that after linearization of equations (1)–(3) we can derive the following dispersion relation:

$$(\omega - k)^2 = \frac{k^2}{k^2 + k_\perp^2}. \quad (11)$$

So, the phase velocity $v_{ph} = \omega/k$ of linear waves lies within the limits

$$1 - 1/k_\perp < v_{ph} < 1 + 1/k_\perp \quad (12)$$

and one can see that the fast solitary wave velocity is always higher and the slow wave velocity is lower than the v_{ph} .

Integrating equation (6) we find the correct solitary wave solution in the implicit form⁴

$$\begin{aligned} \vartheta = & \frac{2}{k_\perp} \ln(V + \sqrt{V^2 + 1}) \\ & + \frac{M}{k_\perp \sqrt{M^2 - 1}} \ln \left(\frac{MV - 1 + \sqrt{(M^2 - 1)(V^2 - 1)}}{M - V} \right), \end{aligned} \quad (13)$$

where $V = k_\perp |v - 2u + 1|/2$. Let us note that the integration constant in (13) is chosen such that $\vartheta(v_{\max}) = 0$, where

$$v_{\max} = 2u - 1 \mp \frac{2}{k_\perp}, \quad (14)$$

that is, the solitary wave velocity u is proportional to its amplitude v_{\max} , but the relation between these two values is quite different from that of KdV solitons. It is necessary to point out that the solution (13) describes electron bunches for both fast and slow solitary waves.

Now let us turn to the direct numerical solution of equations (1)–(3). Main results are presented in Figs. 1–3 where the spatio-temporal dynamics of the electron fluid velocity v and the space-charge density ρ is shown. Numerical simulation^{4,5} demonstrated that during the evolution process of a rather wide class of initial perturbations one or more stable solitary waves arise and they propagate without changing their form or velocity. In Fig. 1 there is an example of the formation of fast space-charge solitary wave and an oscillatory tail of small amplitude. Initial perturbation was

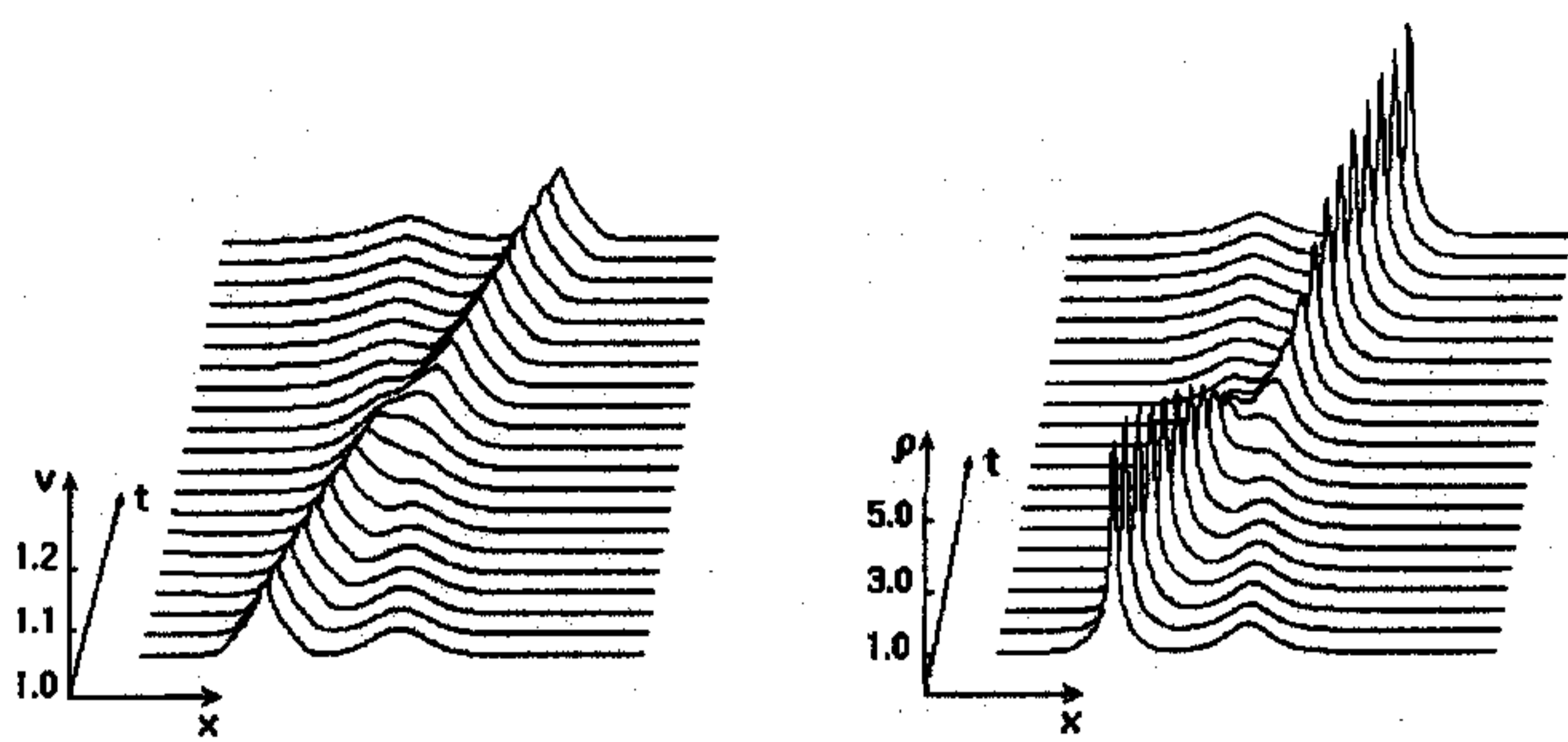


FIG. 2. Elastic collision of two fast solitary waves.

taken to be a half-sine form; the relation between velocity and density perturbation amplitudes was found by solving the linear problem (all results are represented in the beam frame of reference).

We paid special attention to processes of solitary wave collisions. Numerical simulation revealed that overtaking collisions of waves which travel in the same direction when viewed from the beam frame (i.e., collision of two fast or two slow waves) are almost elastic and preserve the waveforms and velocities (Fig. 2). "Head-on" collisions between waves which move in opposite directions (i.e., between fast and slow wave) are essentially unelastic and produces "radiation-like" disturbances (Fig. 3). (The solutions of nonlinear dispersive wave equations usually consist of two parts: solitary waves and weakly nonlinear waves, called oscillatory tails or radiation.⁷)

Now the question is how to treat these results in terms of standard equations or those proposed because of phenomenological reasons? Overtaking collisions can at least be qualitatively described by the KdV equation. Physical processes taking place at head-on collisions are to some extent (but not entirely) in agreement with those described in two papers of Seyler and Fenstermacher^{8,9}. In Ref. 8 an equation (called the symmetric regularized long-wave equation) was proposed for the description of the propagation of weakly nonlinear space-charge waves, which in the beam frame looks as follows:

$$\frac{\partial^2 v}{\partial t^2} - \frac{\partial^2 v}{\partial x^2} + \frac{1}{2} \frac{\partial^2 (v^2)}{\partial x \partial t} - \frac{\partial^4 v}{\partial x^2 \partial t^2} = 0. \quad (15)$$

Equation (15) possesses solitary wave solutions which slightly differ from KdV solitons. Numerical solution

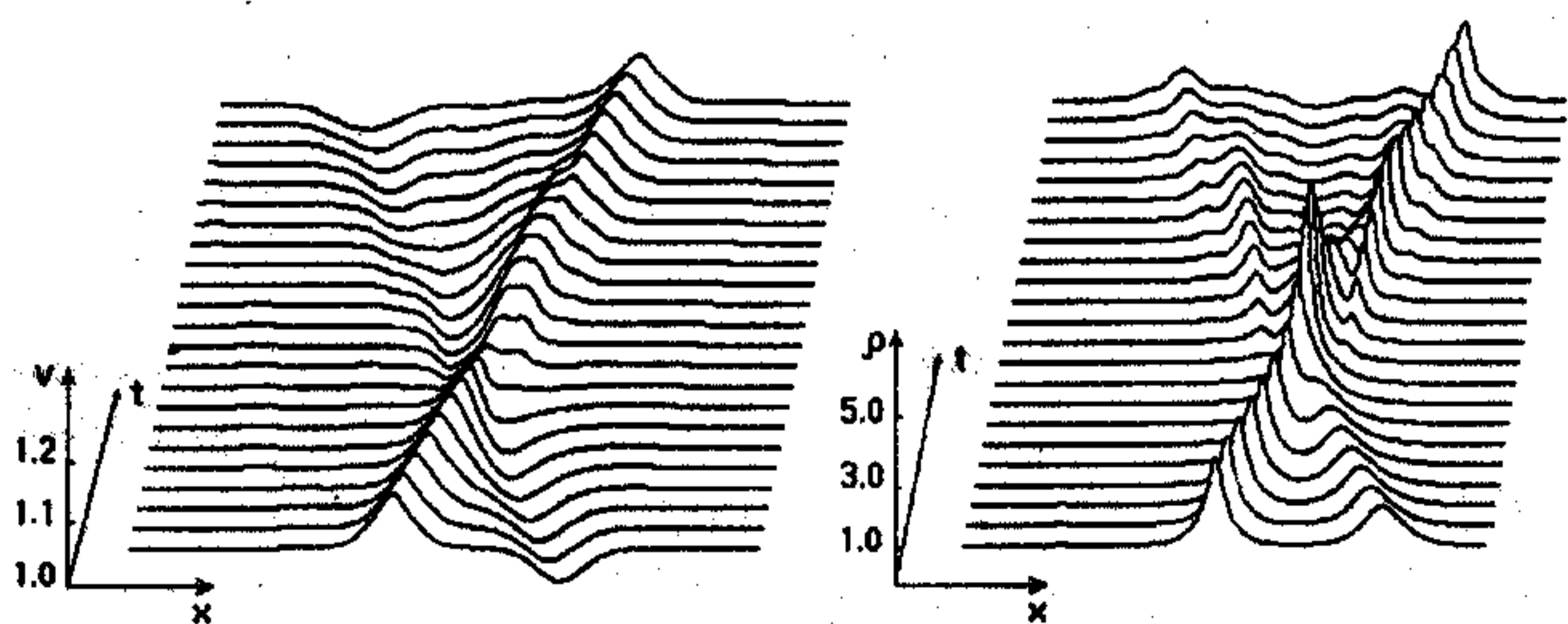


FIG. 3. Unelastic collision between fast and slow solitary waves.

revealed⁸ that solitary waves behave almost elastically in overtaking collisions. "Head-on" collisions were found to be unelastic, but disturbances were observed not only in the form of weakly nonlinear waves but also in the form of one or more (up to eight) additional pairs of solitary waves. In the direct numerical experiments with equations (1) – (3) no new solitary waves appeared, even when amplitudes were close to the breaking conditions.^{4,5} Our analysis showed, that the appearance of additional solitary wave pairs in Ref. 8 occurs at the u values, when wave breaking should take place.

III. PIERCE DIODE—THE SIMPLEST MODEL FOR DISTRIBUTED MICROWAVE ELECTRON SYSTEMS WITH COMPLEX DYNAMICS

The Pierce diode¹⁰ consists of two infinite plane parallel grids pierced by a monoenergetic infinitely wide electron beam with space charge neutralized by an ion background. The grids may be grounded or connected with a circuit containing various passive or active elements. Charge density and electron beam velocity at the input are supposed constant; ion background charge density is equal to the unperturbed electron charge density in the beam. The only parameter of the system is the nonperturbed transit angle with respect to the plasma frequency

$$\alpha = \omega_p d / v_0, \quad (16)$$

where d is distance between grids; v_0 is flow velocity at the input electrode; and ω_p is plasma frequency appropriate to charge density at the system input. In Ref. 10 it was demonstrated for the first time that electron beam motion becomes unstable at $\alpha > \pi$. Charge density fluctuations in the flow cause charge redistribution in the outer circuit, connecting grids, and the appearance of induced charges at the system limiting grids. As a result the potential at the grids is constant and field of induced charges strongly influences the motion of the beam. Instability increases until a region with the value of space-charge potential ϕ close to the cathode potential arises, and a virtual cathode (VC) appears. The VC reflects some part of the electron flow back to the input grid.

The Pierce diode is one of the simplest models of distributed MW electronic systems, which is able to demonstrate almost all types of the complicated dynamics. This system attracts considerable interest because of consideration of deterministic chaos in the Pierce diode^{11,12} as well as in the more general case of charge imbalance at the entrance electrode.^{13,14} For a general view on the various scenarios of transition to chaos in the beam-plasma system see Refs. 15 and 16. The following brief description of the diode dynamics is based on the results of Refs. 17–19.

Equations (1) and (2) are used, and in the case of an infinitely wide beam instead of equation (4) we have

$$\frac{\partial^2 \phi}{\partial x^2} = \alpha^2 (1 - \rho). \quad (17)$$

Now x is referred to d and t – to d/v_0 . The boundary conditions are changed fundamentally. Now they are

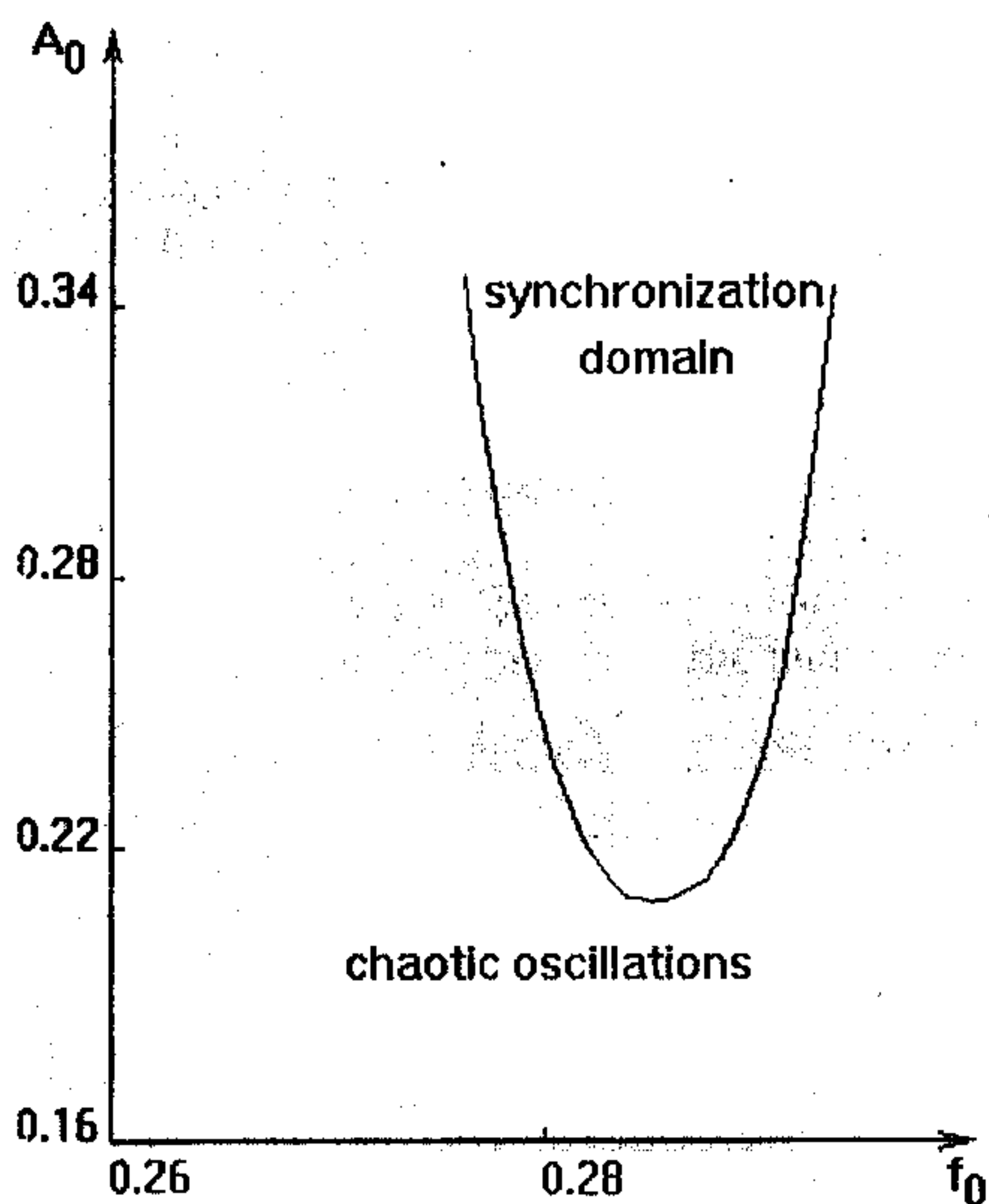


FIG. 4. The synchronization domain for hydrodynamical regime of electron beam in the Pierce diode.

$$v(0,t)=1, \quad \rho(0,t)=1, \quad \varphi(0,t)=0 \quad (18)$$

at the input grid and

$$\varphi(1,t)=0 \quad (19)$$

at the output grid.

The application of the hydrodynamic concept is limited by the condition

$$E_0 > -\alpha, \quad (20)$$

where E_0 is electric field at the system input. One can see from the solution of the stationary nonlinear problem¹¹ that the flow velocity remains a single-valued function only when inequality (20) is satisfied.

When the grids are grounded, a transition to chaos through the Feigenbaum sequence of bifurcation takes place while α decreases. In particular, the value $(\alpha_1 - \alpha_2)/(\alpha_2 - \alpha_3) = 4.63 \pm 0.03$, which is in a good agreement with the value of the Feigenbaum constant $\delta = 4.669 \dots$ ²⁰ In the bifurcation diagram one can see an attractor crisis which arises because of the collision of the attractor with the unstable equilibrium point.^{11,20}

The case where there is a capacity in the outer circuit had been studied in Ref. 20. We studied the dynamics of Pierce diode with other types of passive elements in the outer circuit. When resistance is included the transition to chaos through the Feigenbaum scenario still persists. Increasing the resistance or the inductance leads to decreasing the bifurcation values of α ; the width of α domains, corresponding to regular modes, do not change significantly. At the same time, the chaos threshold shifts in the region of smaller α .

To study the possibility of synchronization of chaotic motion, it was suggested that the boundary condition is $\varphi(1,t) = A_0 \sin(f_0 t)$. It was found that for some values of A_0 and f_0 the strange attractor transforms to the three-loop cycle in the phase space. The synchronization domain is shown in Fig. 4 on plane of parameters A_0 and f_0 , where one

can see a finite synchronization threshold, confirming the dynamic character of chaotic oscillations. Transition to chaos through the period doubling is observed when A_0 becomes lower than the threshold value, as well as when the frequency f_0 is detuned from the synchronization frequency.

What is the physical picture of electron processes in a Pierce diode corresponding to chaotic behaviour? Two, oscillating in space and time, condensations of "electron fluid" occur in the electron flow (they are approximately at $x=0.2$ and 0.8). In the chaotic oscillation regime an initial perturbation grows yet the charge density in the lower condensation still does not exceed some threshold value. After that the strong deceleration field produced by this condensation reduces the flow velocity upstream. Thus, during the time of about d/v_0 the diode loses much more "electron fluid" than flows into it. Further, the instability leads to the increasing of the density perturbation and the process may occur over and over. But because of the difference in the initial conditions the dynamics of the instability limitation is different too. During this cycle the phase trajectory does not come back exactly to its initial position, and, hence, the process does not repeat itself.

A virtual cathode (VC) creates a region of reflected flow and we cannot use a hydrodynamical description. We solved the problem using a PIC-simulation method.²¹ Each particle moves in accordance with the dimensionless equation

$$\frac{d^2 x_i}{dt^2} = -E(x_i), \quad (21)$$

where x_i is the i th particle coordinate, $E(x_i)$ is space charge field at point x_i . The space charge potential is obtained from equation (17).

The numerical experiment helps to reconstruct the picture of the physical processes in the oscillation of the electron beam with a VC. Having appeared, a charge density disturbance leads to decelerating of the electrons entering the system and to increasing the charge density in the perturbation domain. When φ becomes greater than the accelerating voltage reflected electrons appear and the charge density in the VC domain decreases. The latter leads to reducing the decelerating field and to terminating the particle reflection; the system returns to its initial state, and the process described above repeats.

There are three intervals of α values ($1.00 < \alpha/\pi < 1.28$, $1.40 < \alpha/\pi < 1.55$, $1.58 < \alpha/\pi < 1.68$), where VC oscillations are chaotic (the spectrum noise component is rather significant, autocorrelation function decreases, and a strange attractor emerges in the phase space).

The charge density in the flow peaks twice a period. The first higher peak is the result of the Pierce instability development, the second one occurs due to the kinematic electron bunching. Both bunches can easily be recognized on the space-time plot of "electron sheets" motion during one oscillation period (Fig. 5).

Trajectory concentration corresponds to electron bunch formation. Figure 5 demonstrates the VC decay, when some of the electrons are reflected by it, and the others are decel-

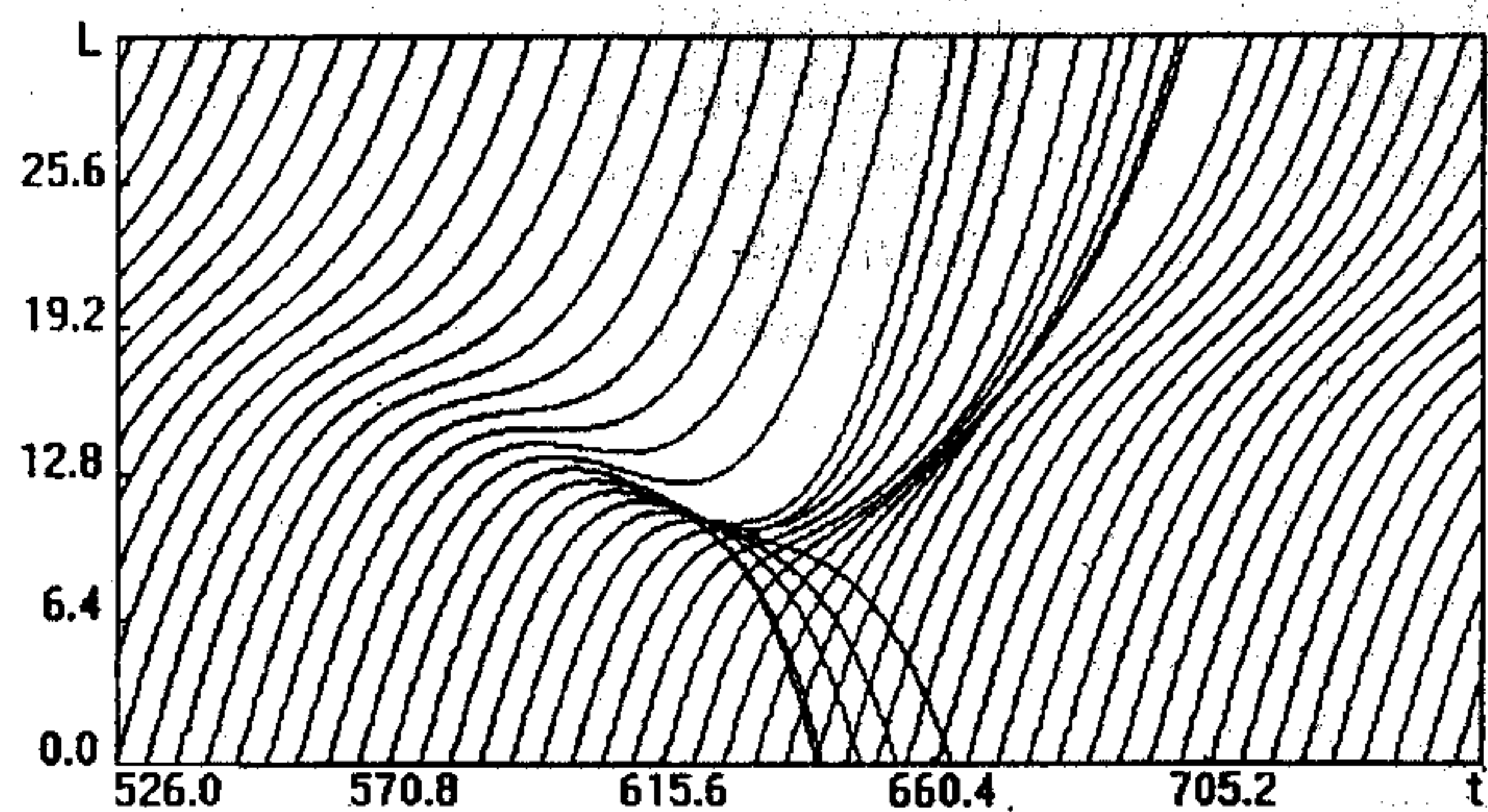


FIG. 5. The trajectory of charged particles during virtual cathode formation.

erated in the VC domain and move towards the output grid. During the VC decay process the charge density and the decelerating field of the VC decrease. So, the velocity of entering electrons becomes greater than that of the electrons which entered the system previously. Such a velocity modulation leads to the formation of an electron bunch moving through the system (the second peak in the time history of the charge density corresponds to this electron bunch).

These two bunches are formed for arbitrary initial conditions. According to Ref. 22, it is possible to speak about the formation of two autostructures in the system under consideration. The dissipation, which is essential for structure formation, is caused by the escaping electrons, which carry away the kinetic energy.

It is demonstrated in Refs. 18 and 19 that strong chaotic oscillations in the electron beam are related to the interaction of structures. In the regular or weakly irregular regimes

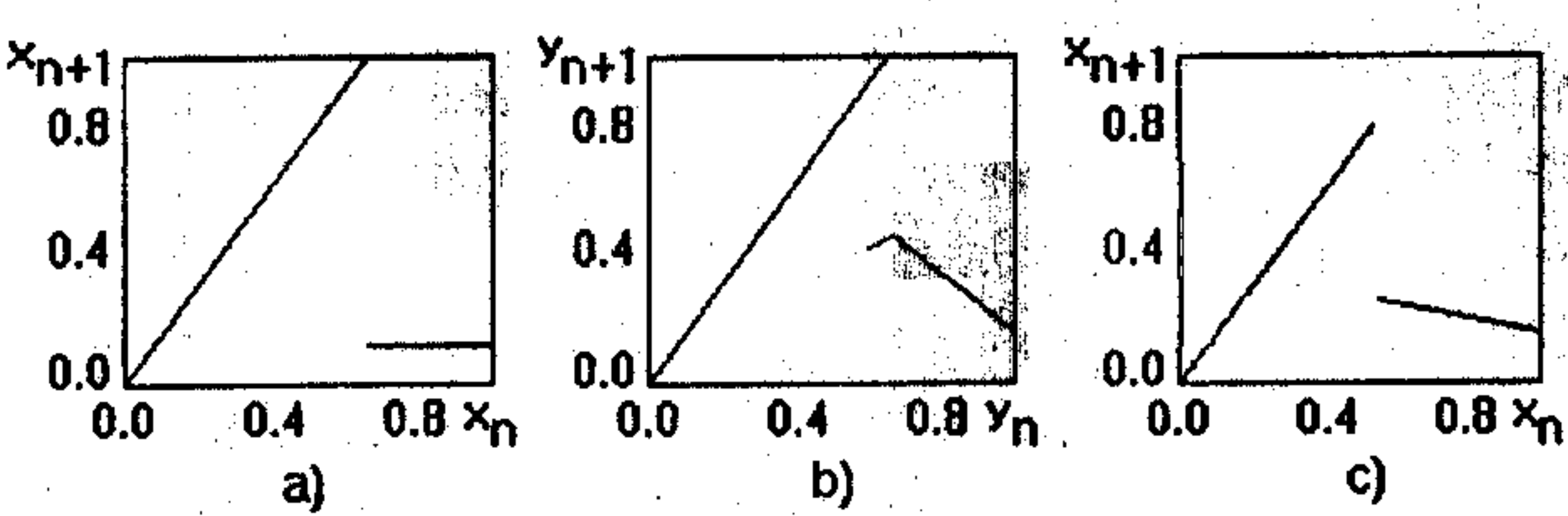


FIG. 6. The maps for charge density in the chaotic regime: (a) for virtual cathode, (b) for second structure and (c) for virtual cathode in the weakly chaotic regime.

structure interaction is realized only through the space-charge field, and the coupling through the flow is not significant. Strongly irregular oscillations appear when the charge density in the second electron bunch increases so that some electrons can be reflected by it. This reflected flow defines the initial conditions for VC formation (in the phase space the trajectory moves from the rarely attended attractor region which corresponds to the reflection from the second bunch).

In Ref. 19, a simple model of the system in the form of two coupled maps was proposed as a result of the analysis of the charge density time histories in each structure. The distributed nature of the system is not considered in the model, but it can describe instability and nonlinearity, leading to structure formation, as well as coupling between the structures.

The first map (with regular dynamics) describes the relationship between the values x_{n+1} and x_n of the charge density in the VC domain at sequential time points (Fig. 6a):

$$x_{n+1} = \begin{cases} ax_n, a > 1 & \text{—charge density increase on the VC, when } x_n < x_{cr}, \\ \text{const} & \text{—charge density increase limitation, at } x_n > x_{cr}, \end{cases} \quad (22)$$

where x_{cr} is the charge density value in the VC domain at which the limitation takes place.

The second map describes the charge density y_{n+1} to y_n at sequential time points in the second structure (Fig. 6b) and can be put as follows:

$$y_{n+1} = \begin{cases} ay_n, a > 1 & \text{—charge density increases in the electron bunch, at } y_n < y_{cr1}, \\ b_1y_n + b_2 & \text{—charge density decrease because of escaping} \\ & \text{of the bunch from VC domain at } y_n < y_{cr2}, \\ c_1y_n + c_2 & \text{—charge density increase limitation because of reflecting} \\ & \text{of some electrons from the bunch at } y_n > y_{cr2}, \end{cases} \quad (23)$$

where y_{cr1} is the charge density in the second bunch after modulation and y_{cr2} is the threshold of charge density limitation.

Structure coupling in the flow is considered as follows: the charge density value in the VC domain sets initial con-

ditions for the second map, and the charge density in the part of the beam reflected from the second structure is added to the charge density in the VC domain after the limitation. Decreasing of the control parameter y_{cr2} provides coupling between the structures, leading to transition to chaos through

intermittency (this result coincides with the "particles-in-cell" simulation).

Weakly chaotic oscillations at the VC are not caused by the interaction of the structures. The instability is determined by the connection between the charge density in the VC domain during formation and the same after limitation. This corresponds to the negative slope of the second part of the first map at $x_n > x_{cr}$ (Fig. 6c).

IV. A FURTHER IDEA OF NONLINEAR DYNAMICS APPLIED TO VACUUM MICROELECTRONICS

As soon as a new active element appears in electronics, one thinks first of all about the construction of an oscillator. One of these new elements is a field emission microtriode. Its nonlinear character is defined by the Fowler-Nordheim law (see Ref. 23 for example). An oscillator based on such an element is of great interest in the rapidly developing field of vacuum microelectronics, in particular, because the microtriode can operate at microwave frequencies.

It is possible to construct such an oscillator using positive feedback in the microtriode amplifier (as in conventional vacuum-tube oscillators). However, because of the absence of current saturation, an infinite growth of oscillation amplitude would be observed in this oscillator, which would cause the cathode destruction at a high current density. To compensate the amplitude growth it is necessary to insert a dissipative element with nonlinear characteristics into the feedback circuit. When the amplitude is less than the threshold A , a nonlinear dissipation does not compensate the instability defined by the nonlinearity of the active element, and when the amplitude values are greater than A , dissipation leads to the oscillation amplitude saturation.

The analysis of this oscillator is also interesting from the viewpoint of constructing an active nonlinear medium-model, because it is known that the simplest medium-model is a chain (or lattice) of coupled oscillators (see Refs. 24 and 25, for example).

There are two approaches to the investigation of this oscillator. The first approach is the derivation of a mathematical model and its numerical investigation. The second one is the construction of a radiotechnical model-analog. Using the second approach, many nonlinear phenomena in active media had been investigated experimentally on the LC transmission lines: space competition of the waves, explosive instability, generation of stationary waves at high-frequency and low-frequency waves interaction, and so on (see Ref. 25, for example).

The plan of our oscillator is shown in Fig. 7. The oscillator consists of a field emission microtriode, a nonlinear RLC -circuit (nonlinearity is determined by a resistor R), and an inductive feedback. The anode current value depends on the grid voltage according to the Fowler-Nordheim law:^{26,27}

$$I_a = AF^2(aU + b)^2 \exp(-B\Phi^{3/2}/(F(aU + b))), \quad (24)$$

where I_a is the anode current, U is the grid voltage, A and B are nearly constant parameters, Φ is the emitter work function, F is the field-enhancement factor, and a and b are

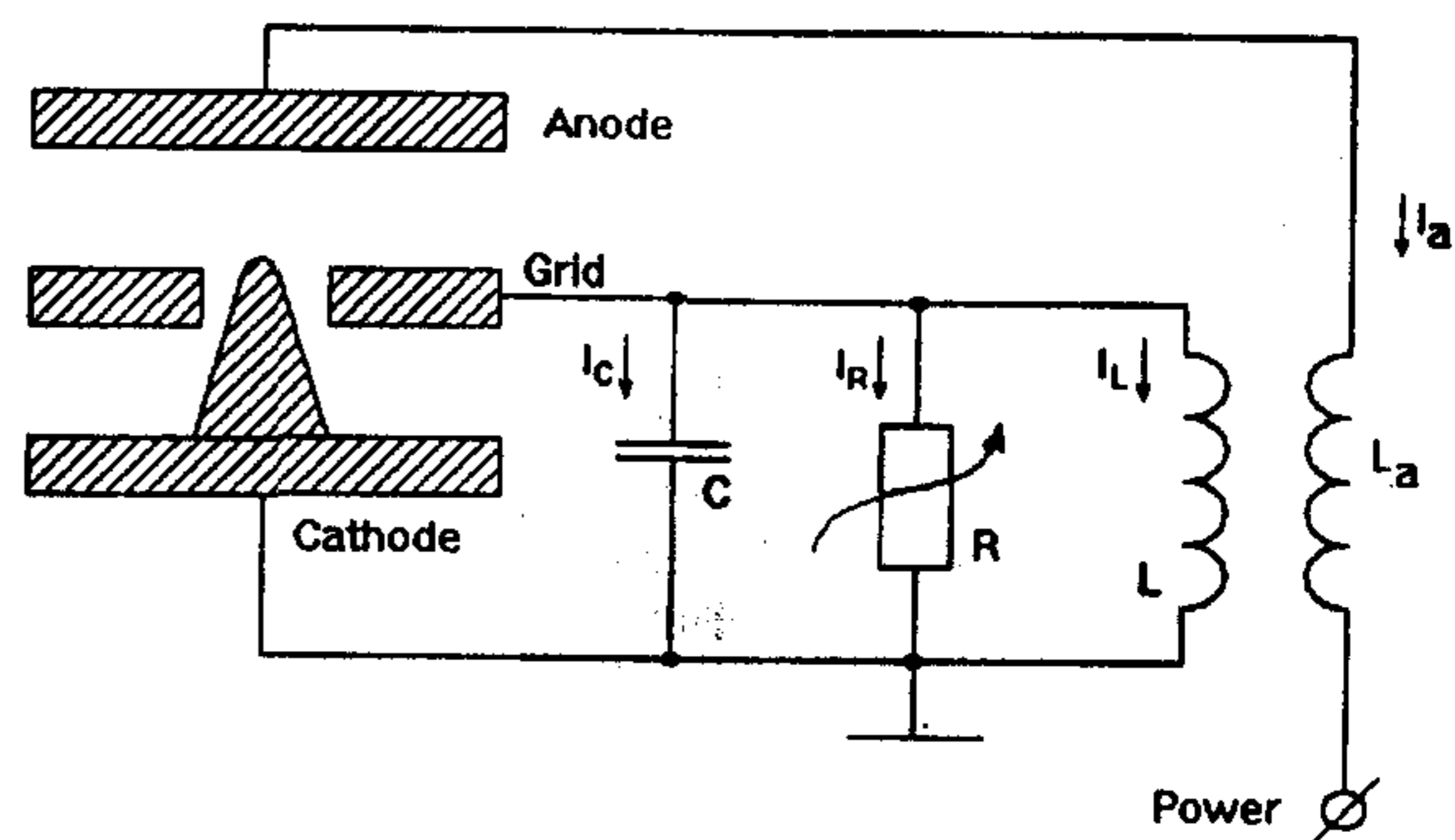


FIG. 7. The experimental scheme of the oscillator, based on a field emission microtriode.

geometric constant values. We used parameter values and designations from Refs. 26 and 27. It is possible to demonstrate that I_a depends on the grid voltage U exponentially at $U > -b/a$.

Nonlinear dissipation is determined by the current-voltage characteristic of the resistor R :

$$I = I_0[\exp(U/U_0) - 1], \quad (25)$$

where I is the resistor current, U is the resistor voltage, and I_0 and U_0 are resistor parameters. Let us notice that the theoretical current-voltage characteristic of a semiconductor diode has the form of equation (25) where I_0 is the theoretical reverse diode current, $U_0 = kT/e$ is the thermal potential, k is the Boltzmann constant, T is the temperature in Kelvin, and e is the electron charge. The oscillator equation with dimensionless variables takes the form:

$$\begin{aligned} & \frac{d^2x}{d\tau^2} + (g_0 \exp(kx)) \\ & - \mu(2x + 2\sigma + 1)\exp(-1/(x + \sigma)) \frac{dx}{d\tau} + x \\ & = \begin{cases} 0, & \text{autonomous mode,} \\ V \sin(p\tau), & \text{non-autonomous mode.} \end{cases} \end{aligned} \quad (26)$$

The following dimensionless variables are introduced into equation (26): x is the grid voltage, g_0 and k are nonlinear resistor parameters, μ is the coupling coefficient, σ is the nonlinearity parameter, V and p are amplitude and frequency of external force, and τ is the time.

It is obvious that equation (26) differs significantly from the classical Van der Pol or Rayleigh equations (see Ref. 24, for example).

The radiotechnical model (see Fig. 8) includes the LC -circuit with nonlinear dissipation (diodes D) and the nonlinear amplifier 2 having the exponential characteristic. The feedback is closed through coupling transformer consisting of inductors L_1, L_2 . The linear amplifier 1 serves to apply the external harmonic drive. The nonlinearity parameter is tuned by varying the gain of the exponential amplifier and dissipation is varied by changing the number of diodes in the circuit. The feedback coefficient is fixed.

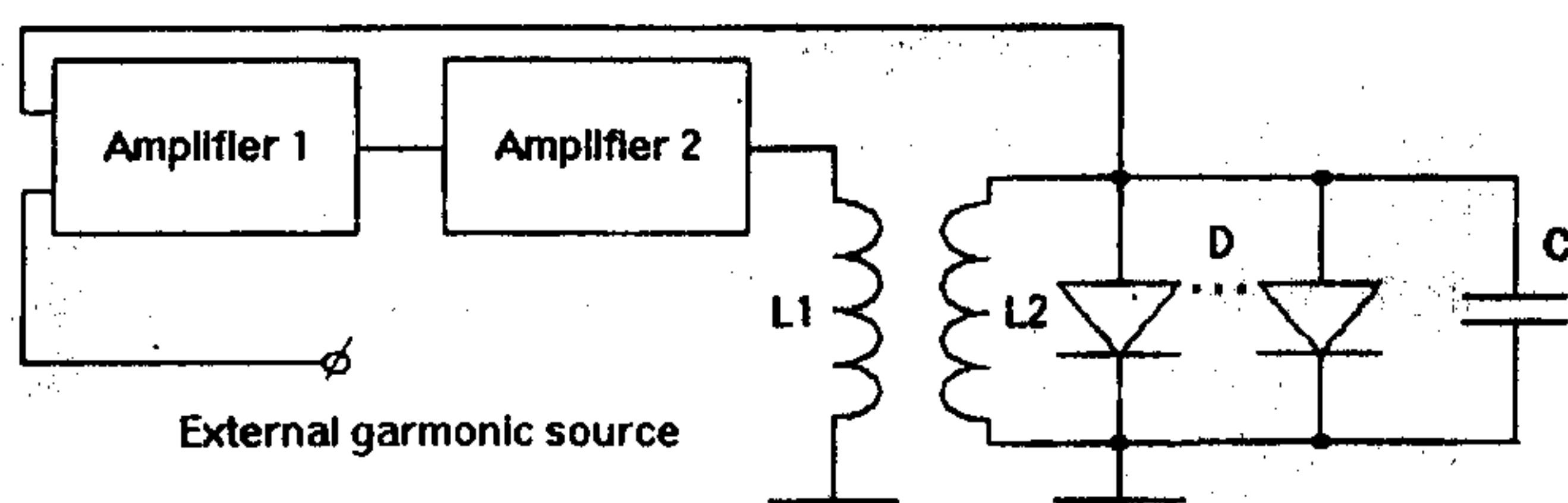


FIG. 8. The radiotechnical model of the oscillator.

In experiments with the model-analog, the types of behaviour were recognized using time series, phase portraits and power spectra. The time series were observed on the oscillograph screen and recorded in a computer. To obtain the phase portrait, we apply the voltage time series from the nonlinear amplifier output to the first oscillograph input. The same signal after passing through the RC -filter is applied to the second input of the oscillograph.

Experimental investigation of the autonomous oscillator demonstrated that the soft and hard self-excitation of oscillations is possible (limit cycle is obtained). With nonlinearity parameter growth, the size of the limit cycle increases and its shape deforms.

In the nonautonomous mode we investigated the radiotechnical model-analog by varying the amplitude and frequency of the external harmonic source for different nonlinearity parameter values.

We observed the following dynamics: for low values of the nonlinearity parameter the oscillator demonstrates either quasiperiodic oscillations with two incommensurable frequencies or resonance on torus (synchronization tongues) when the amplitude and the frequency of the external force are varied. When the nonlinearity parameter increases, the synchronization tongues overlap. The behaviour in overlapping regions corresponds to the transition to chaos by intermittency. Inside the synchronization tongues a transition to chaos through the period doubling is observed.

Topography of the parameter plane for the experimental system, when the nonlinearity parameter is sufficiently large, is shown in Fig. 9. The horizontal axis corresponds to external force frequency, normalized to the self-oscillation fre-

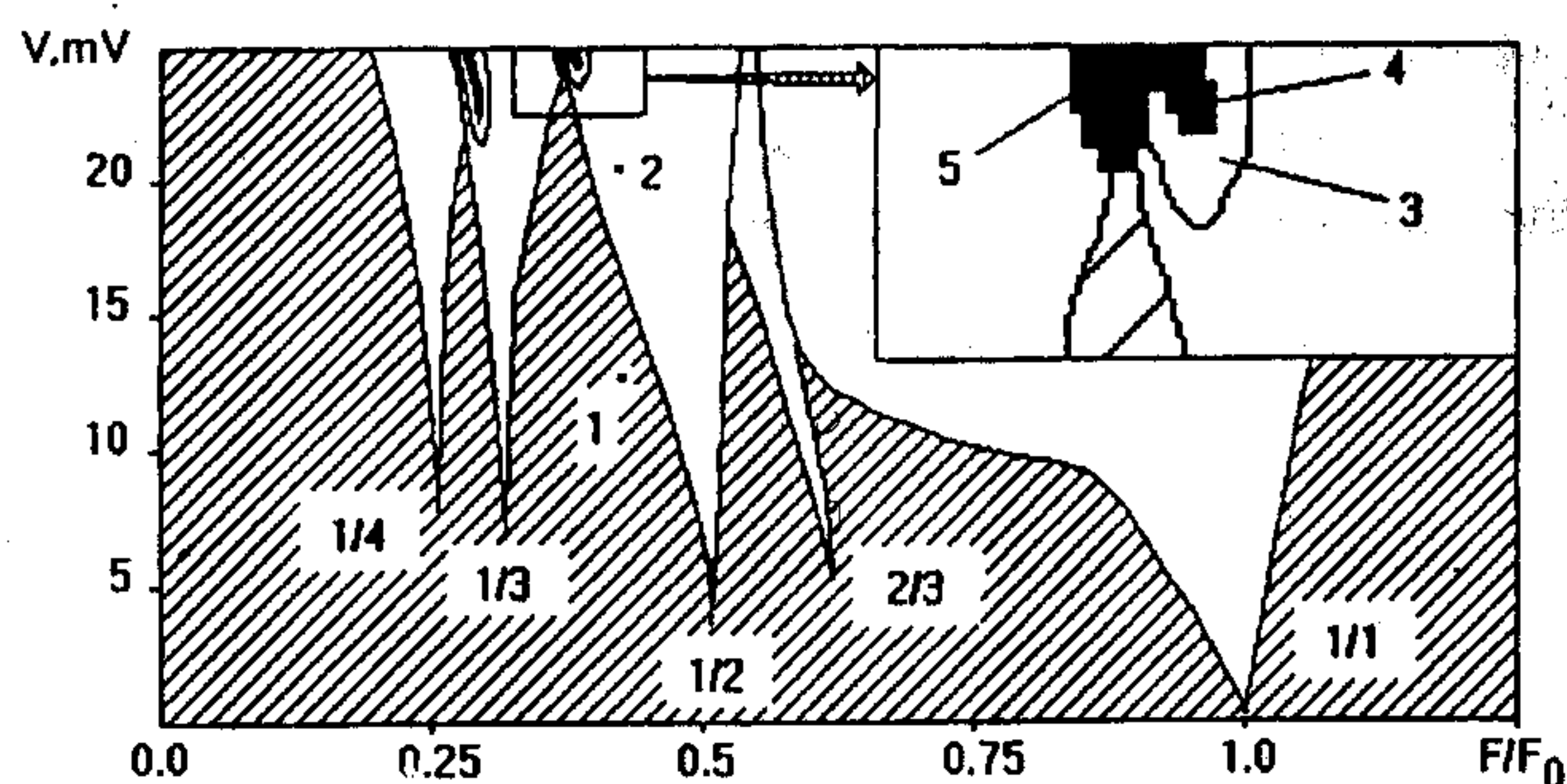


FIG. 9. Topography of the parameter plane of amplitude-frequency external force for experimental system.

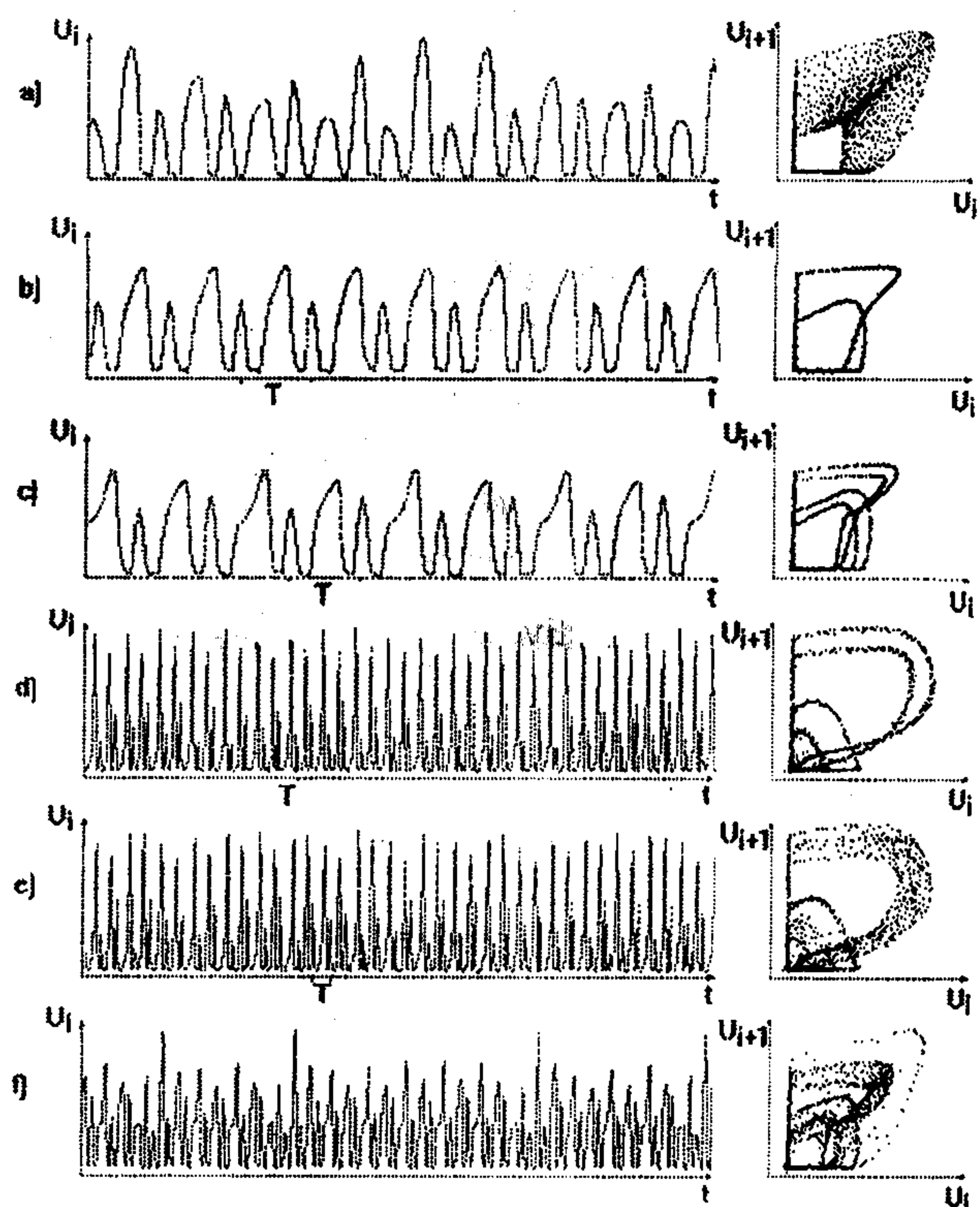


FIG. 10. The discrete time series of processes in radiotechnical model and phase portrait projections: (a) quasiperiodical regime, (b) resonance cycle, (c) doubled resonance cycle, (d) weakly chaotic regime, (e) chaos, (f) intermittency regime.

quency of radiotechnical model-analog at a fixed nonlinearity parameter. The vertical axis corresponds to the amplitude of external force in millivolts. Quasiperiodicity regions are shaded. The boundaries of regions of the resonant cycles are shown by continuous lines. The fractional numbers correspond to the resonance numbers. The continuous lines inside the synchronization tongues bound a region where period doubling bifurcations and transition to chaos take place. Chaos regions are painted in black.

Figure 10 shows the discrete time series of processes in our radiotechnical model [$U_i = U(t_i)$ dependence] and phase portrait projections [$U_{i+1} = f(U_i)$ dependence]. Here U_i are the sampled values of the voltage from the output of the nonlinear amplifier, recorded into the computer using an analog-digital converter.

Figure 10a illustrates a quasiperiodic motion. This mode corresponds to point 1 in Fig. 9. The time series show that the analyzed process has two incommensurable frequencies which are the self-oscillation frequency of the radiotechnical model-analog and the modulation frequency.

Figures 10b,c correspond to the appearance of a resonant cycle on the torus with the rotation number $1/2$ and its period doubling (points 2,3 in Fig. 9). The period of the external drive is denoted by T .

Only one period doubling bifurcation is usually observed in the experiment. After this bifurcation, transition to chaos (Fig. 10d) and merging of the attractor bands take place (Fig.

10e). The time series in Fig. 10d is chaotic (point 4 in Fig. 9). This fact manifests itself in the “thickening” of the phase portrait projection, but the rough structure of the resonant cycle is still preserved. When the merging of the attractor bands takes place, this structure is destroyed. The transition to chaos after only one period doubling bifurcation of a resonant cycle occurs possibly, because of the strong dependence of the system on internal noise. The latter is associated with the exponential form of the current-voltage characteristic of the nonlinear element.

Figure 10f demonstrates the time series and phase portrait projections which could be considered as transition to chaos through intermittency (point 5 in Fig. 9) so the time series gives nonperiodic bursts. The phase portrait projection has two distinct parts: an outer part corresponding the time series bursts, and an inner part which is close to the structure of the attractor corresponding to the period doubling route to chaos. The numerical simulation results are in qualitative agreement with the experimental ones.

V. PHENOMENOLOGICAL ELECTRON TURBULENCE PATTERN MODEL (EMISSION IN CONNECTED SMALL VOLUME CHAINS CONTAINING ELECTRON OSCILLATORS)

Phenomenological models, created first of all to explain turbulence phenomenon, occupy an important part in nonlinear dynamics. In particular, a turbulence model arising in hydrodynamic flow by the formation of interacting coherent structures should be mentioned.²⁸ In microwave electronics the structure formation in electron flows had been observed experimentally by the authors of Ref. 29. The appearance of the chaotic oscillations had been found experimentally in a tubular annular electron flow drifting in a longitudinal constant magnetic field,³⁰ and it had been suggested that the complex dynamics of the flow had been caused by the electron structures interaction. In our works^{31,32} we considered the following phenomenological model of electron flow beginning with the stage when the structures have sprung up.

Let us admit that there is a sequence of electron structures affecting each other. Suppose that the structures are small volumes of the active medium consisting of electron oscillators. It can be assumed that superradiance takes place in every electron ensemble (see Refs. 33 and 34, for example). This superradiance arises as a result of oscillator interaction via the field of their radiation and phase focusing. Processes in the flow of interacting electron ensembles are described by the set of dimensionless differential equations³¹

$$\dot{c}_{ki} + j\theta(|c_{ki}|^2 - 1)c_{ki} = -\bar{c}_i + K_F\bar{c}_{i-1} + K_B\bar{c}_{i+1}, \quad (27)$$

where $k=1, \dots, M$; $i=1, 2, 3, \dots$; M is electron number in each ensemble; c_{ki} is the dimensionless complex variable corresponding to the k th electron field in the i th structure; $\bar{c}_i = (1/M) \sum_{k=1}^M c_{ki}$ defines the dipole momentum of the i th electron system; the θ parameter is proportional to the ratio of the coefficient of nonisochronism to the electron dis-

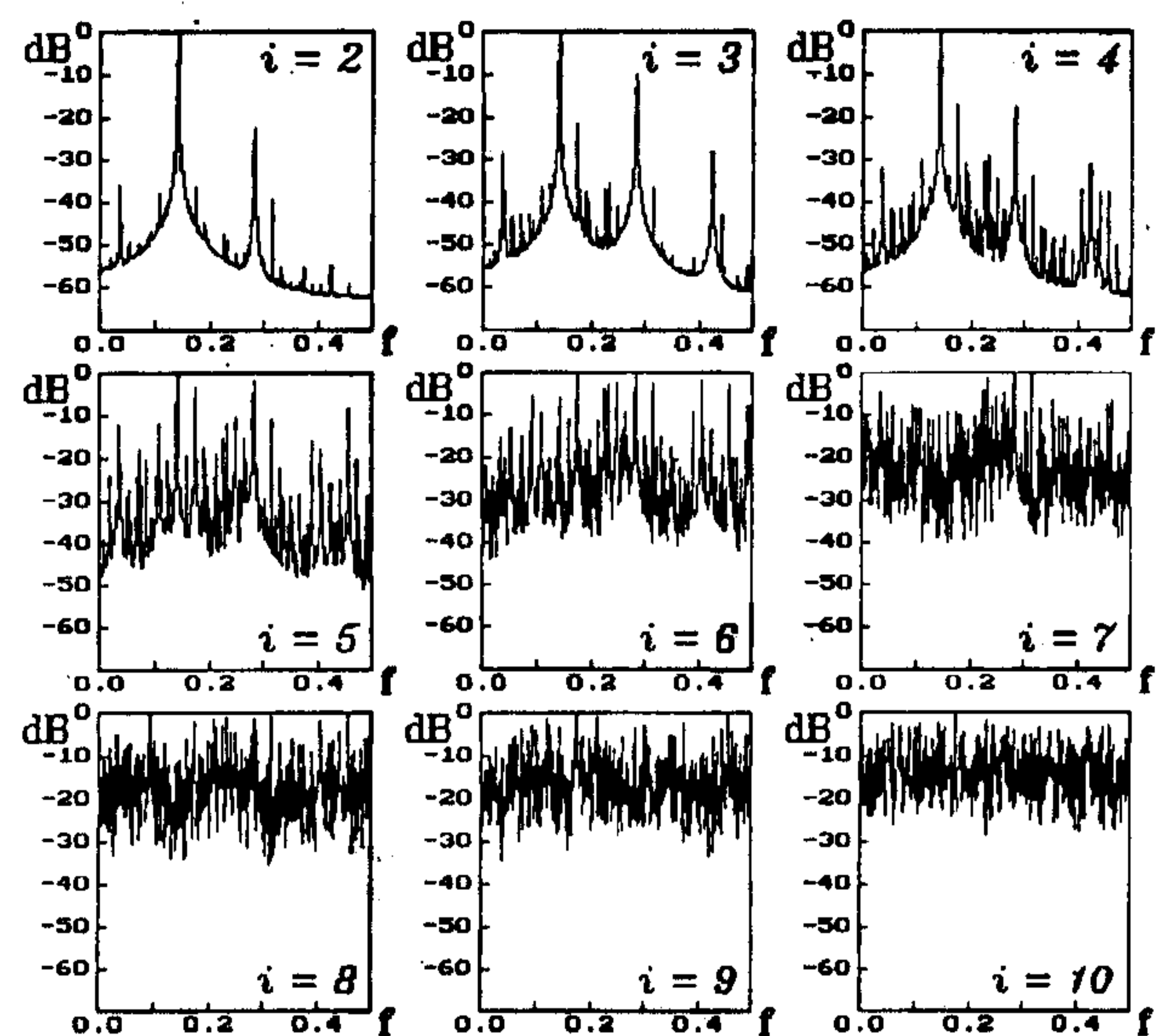


FIG. 11. Power spectra for time series, given by equation (27)

sipation factor³³; K_F and K_B are the coefficients of mutual influence of the structures; and the dot denotes differentiation on the dimensionless time.

We have solved the equation (27) numerically under the assumption that at the initial time a weak perturbation of electron phases δ had been introduced, that is, at the initial time:

$$c_{ki} = \exp \left[-j \left(\frac{2\pi k}{M} + \delta \cos \frac{2\pi k}{M} \right) \right]. \quad (28)$$

Electron structures motion fits the “transfer of information” from $(i-1)$ th to i th section of the flow in a time $\Delta t = \Delta T/N$, where N is the number of structures simultaneously present in the flow, and ΔT is the time of radiation of a single electron volume which approximately corresponds to the structures “lifetime” in the interaction space.

Figure 11 demonstrate a rather noticeable complication of the spatio-temporal dynamics of the flow of coherent electron structures: the temporal regularity breaks with the increasing of the discrete spatial coordinate i . Let us notice that there is a large number of parameters which strongly influence the behaviour of the system and the field distribution (see Ref. 31).

Let us complicate the model. Suppose now that the structures pass through the chain of identical uncoupled cavities. Let the electron structures stay in each of them for a time T which is sufficient for the electrons to interact with the cavity field. This model may be described by the following system of equations³²:

$$\dot{c}_{kn} + j\tilde{\theta}(|c_{kn}|^2 - 1)c_{kn} = jc_{ri}, \dot{c}_{ri} + j\xi c_{ri} = j\bar{c}_n, \quad (29)$$

where c_{ri} is dimensionless complex variable, corresponding to the i th cavity field; c_{kn} corresponds to the field of the k th electron in the n th structure; $\bar{c}_n = (1/M) \sum_{k=1}^M c_{kn}$ is the averaged field of the n th structure; $\tilde{\theta}$ is a ratio of the noniso-

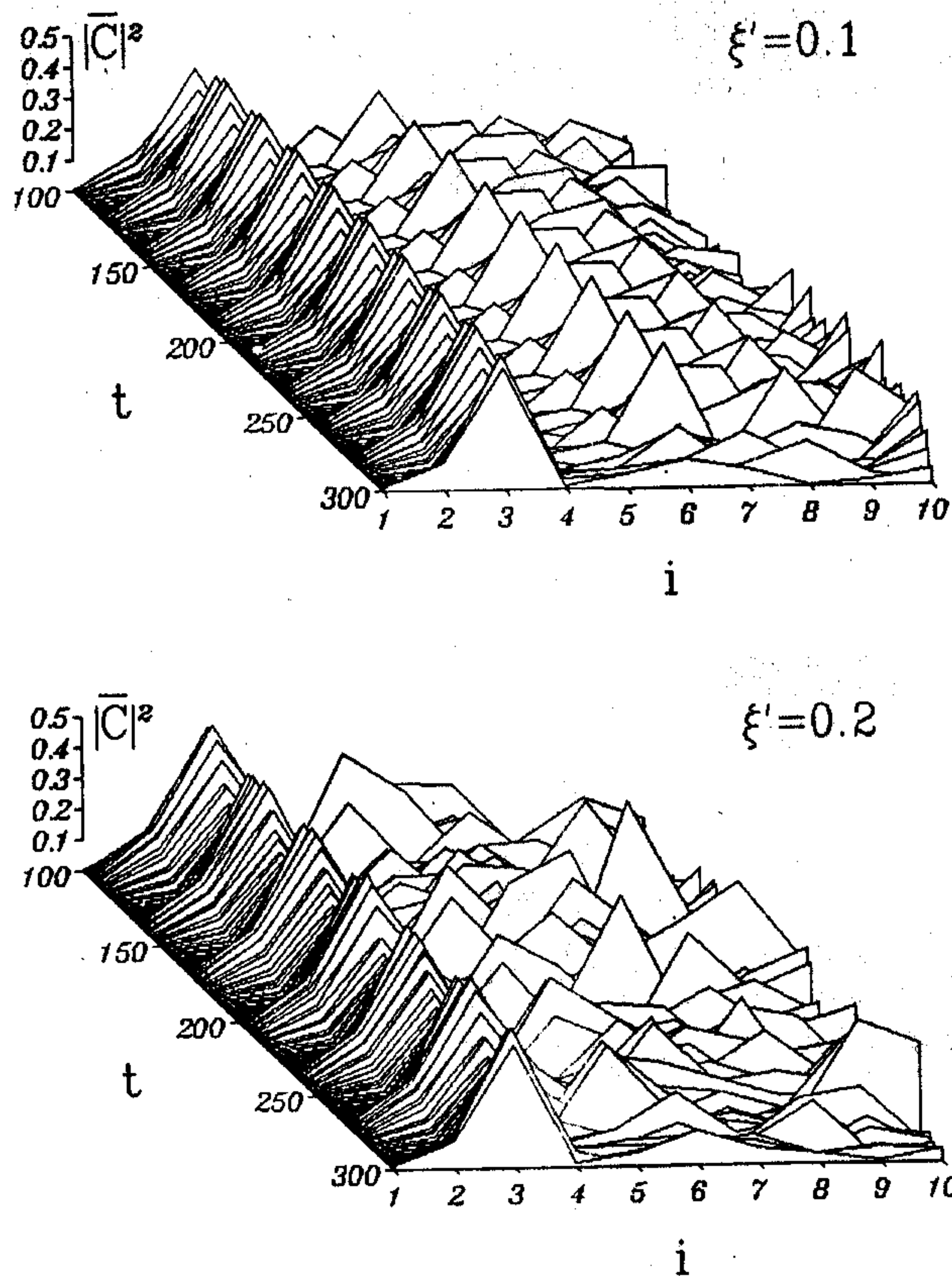


FIG. 12. Spatio-temporal distribution of the radiation field for the flow interacting with two cavities for different values of frequency ξ' .

chronism coefficient to the amplification parameter³²; and $\xi = \xi' - j\xi''$ is the dimensionless complex resonant frequency of the cavity.

For the n th electron structure entering the flow the initial conditions are

$$c_{kn}(0) = \exp\left(-j \frac{2\pi k}{M}\right). \quad (30)$$

The system of equations (29) is solved during the time T when the n th structure passes through the i th cavity. After the time T the n th electron structure enters the $(i+1)$ th resonator and since that time the variables $c_{r_{i+1}}$ should be used in equations (29). At the same time the $(n-1)$ th structure enters the i th resonator instead of the n th one, and so on.

First we consider the flow passing through one cavity situated at its beginning ($i=2$) and the other near the end ($i=10$). The results corresponding to this case are shown in Fig. 12. Depending on the value of ξ' , the process looks either more ordered ($\xi'=0.1$) or more chaotic ($\xi'=0.2$). The ordering occurs when ξ' is close to the fundamental frequency of the flow in the absence of cavities which is about 0.14 (Fig. 11). At ($\xi'=0.2$) there is no resonant interaction and the influence of the cavities leads only to phase defocusing. Thus we have a more complicated distribution of $|c|^2$ in time and space.

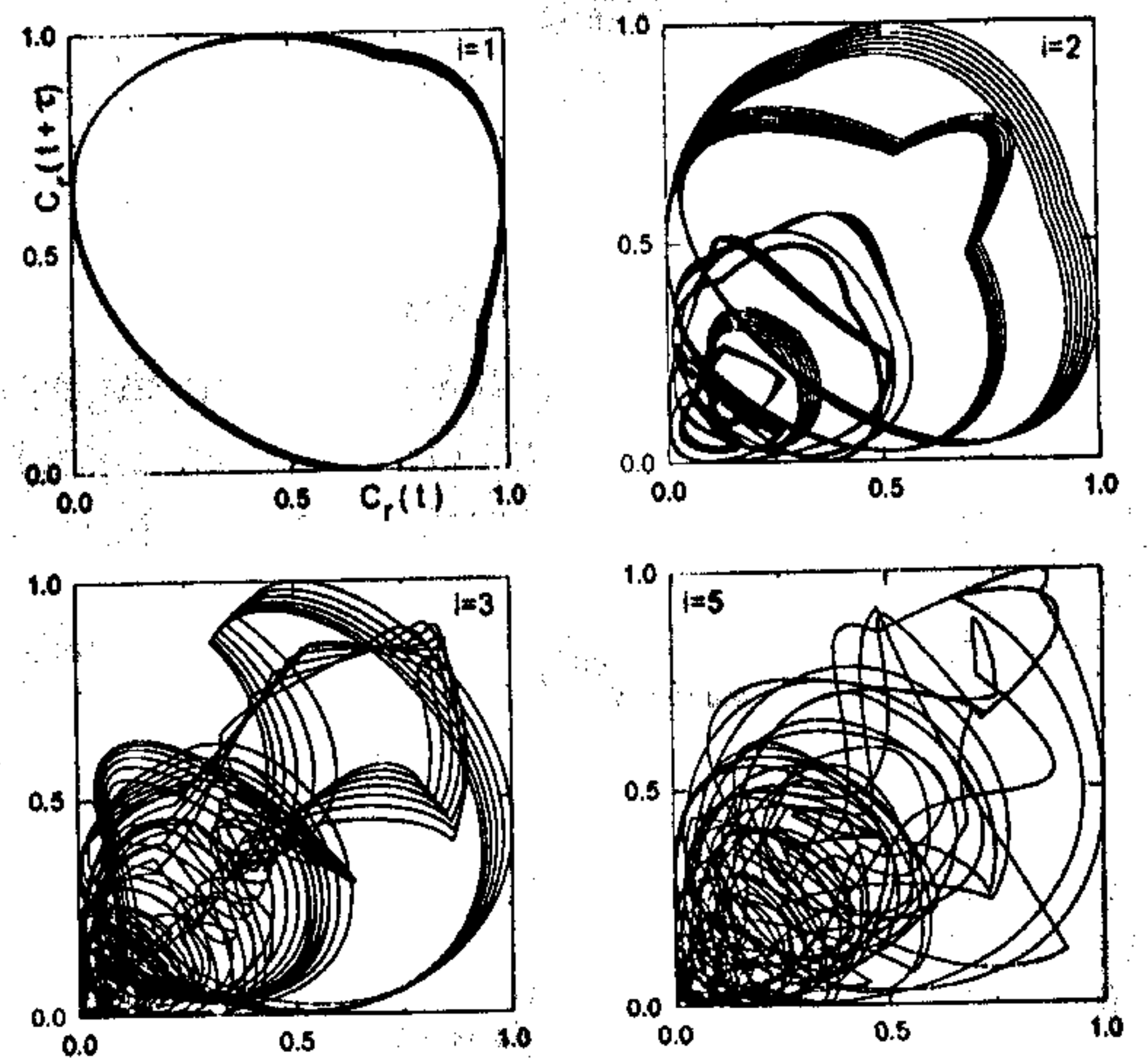


FIG. 13. Phase portraits for the flow interacting with the chain of ten cavities.

Now let us consider a chain consisting of ten cavities. Phase portraits (Fig. 13) reconstructed from realizations for the fields of the first, second, third and fifth cavity show the decay of periodic oscillations with the increasing of i , which corresponds now to the cavity number. Calculations show that initially optimal phase distribution of oscillators breaks when i increases. Such a mechanism destroys the periodical nature of energy interchange between electrons and cavity fields. This is the cause of rather complicated irregular behaviour of the function $|c_r|^2(i, t)$.

VI. SUMMARY

Let us point out once again, that though this paper is devoted to peculiarities of nonlinear interaction of electron flows with microwave electromagnetic oscillations and waves, it was an attempt to show the way of application of nonlinear dynamics ideas and methods in microwave electronics. So, nonlinear dynamics specialists should pay attention to an interesting field of application, namely microwave electronics. As far as electronic specialists are concerned, the following verse by Alexander Kushner holds true for them:

The aspect takes into account very few
But at a closer look it is extremely new.

ACKNOWLEDGMENT

This work was supported by the Russian Basic Research Foundation, Grant No. 96-02-16753.

- ¹W. Louisell, *Coupled Mode and Parametric Electronics* (Wiley, New York, 1960).
- ²J. Rowe, *Nonlinear Electron-Wave Interacting Phenomena* (Academic, New York, 1965).
- ³N. M. Ryskin and D. I. Trubetskov, "Nonlinear electron waves. Methods and results for O-type devices (the review)," *J. Commun. Technol. Electron.* **38**(6), 95–110 (1993).
- ⁴N. M. Ryskin, "Solitary space charge waves," *Izv. VUZov - PND*, **2**(5) 84–91 (1994) (in Russian).

- ⁵N. M. Ryskin, "Interaction of solitary space charge waves," *Pis'ma Zh. Tekh. Fiz.* **20**(17), 1–5 (1994) (in Russian).
- ⁶B. N. Rutkevich, A. V. Pashchenko, V. D. Fedorchenko, and Yu. P. Mazalov, "Steady state waves in the bounded plasma," *Zh. Tekh. Fiz.* **47**(1), 112–124 (1977) (in Russian).
- ⁷A. Newell, *Solitons in Mathematics and Physics* (SIAM, New York, 1982).
- ⁸C. Seyler and D. Fenstermacher, "A symmetric regularized long-wave equation," *Phys. Fluids* **27**, 4–16 (1984).
- ⁹D. Fenstermacher and C. Seyler, "Nonlinear space-charge wave propagation on thin annular electron beams," *Phys. Fluids* **27**, 1808–1818 (1984).
- ¹⁰J. Pierce, "Limiting currents in electron beam in presence of ions," *J. Appl. Phys.* **15**, 721–736 (1994).
- ¹¹B. B. Godfrey, "Oscillatory nonlinear electron flow in Pierce diode," *Phys. Fluids* **30**, 1553–1568 (1987).
- ¹²B. B. Godfrey, "Migma early time density profiles," *Phys. Fluids B* **3**, 1186–1192 (1991).
- ¹³P. A. Lindsay, X. Chen, M. Xu, "Plasma-electromagnetic field interaction and chaos," *Int. J. Electron.* **79**, 237–250 (1995).
- ¹⁴X. Chen, P. A. Lindsay, "Investigation of oscillations and chaos in a plasma-filled diode," *Proc. SPIE* **2557**, 88–97 (1995).
- ¹⁵M. Horhager and S. Kuhn, "Weakly nonlinear steady-state oscillations in the Pierce diode," *Phys. Fluids B* **2**, 2741–2751 (1990).
- ¹⁶C. S. Kueny and P. J. Morrison, "Nonlinear instability and chaos in plasma wave-wave interactions," *Phys. Plasmas* **2**, 1926–1931 (1995).
- ¹⁷V. G. Anfinogentov and D. I. Trubetskov, "Chaotic oscillations in the hydrodynamical model of the Pierce diode," *J. Commun. Technol. Electron.* **38**(4), 106–112 (1993).
- ¹⁸V. G. Anfinogentov, "Chaotic oscillations in the electron beam with virtual cathode," *Izv. VUZov - PND* **2**(5), 69–83 (1994) (in Russian).
- ¹⁹V. G. Anfinogentov, "Coherent structure interaction and chaotic behaviour in the electron beam with virtual cathode," *Pis'ma Zh. Tekh. Fiz.* **21**(5), 70–76 (1995) (in Russian).
- ²⁰W. S. Lawson, "The Pierce diode with an external circuit. II. Chaotic behavior," *Phys. Fluids B* **1**, 1493–1507 (1989).
- ²¹C. K. Birdsall and A. B. Langdon, *Plasma Physics via Computer Simulation* (McGraw-Hill, New York, 1985).
- ²²A. V. Gaponov-Grekhov and M. I. Rabinovich, "Autostructures. Chaotic dynamics of the ensembles," in *Nonlinear Wave. Structures and Bifurcations* (Nauka, Moscow, 1987), pp. 7–44 (in Russian).
- ²³C. A. Spindt, G. E. Holland, and R. D. Stowell, "Field emission cathode array development for high-current density applications," *Appl. Surf. Sci.* **16**, 168–276 (1983).
- ²⁴M. I. Rabinovich and D. I. Trubetskov, *Oscillations and Waves in Linear and Nonlinear Systems* (Kluwer Academic, Dordrecht, 1989).
- ²⁵S. V. Kiashko, "Investigation of nonlinear interactions in the radiowave distributed systems," *Candidat Thesis*, Gorky, 1980 (in Russian).
- ²⁶W. J. Orwis, C. F. McConaghy, D. R. Ciarlo, J. H. Yee, and E. W. Hee, "Modeling and fabricating micro-cavity integrated vacuum tubes," *IEEE Trans. Electron Devices* **ED-36**, 2651–2658 (1989).
- ²⁷T. Asano, "Simulation of geometrical change effects on electrical characteristics of micrometer-size vacuum triode with field emitters," *IEEE Trans. Electron Devices* **ED-38**, 2392–2394 (1991).
- ²⁸A. V. Gaponov-Grekhov, M. I. Rabinovich, and I. M. Starobinets, "The dynamical model of the space development of turbulence," *Pis'ma Zh. Eksp. Teor. Fiz.* **39**, 561–565 (1984).
- ²⁹R. L. Kuhl and H. F. Webster, "Breakup of hollow cylindrical electron beams," *IRE Trans. ED-3*, 172–183 (1956).
- ³⁰V. R. Ampilogova, A. V. Zborovskiy, D. I. Trubetskov, and K. V. Hudzik, "On test of one hypothesis of chaos arising from structures in the electron beam," in *Lectures on Microwave Electronics and Radiophysics* (Saratov University Press, Saratov, 1989), Book 1, pp. 106–110 (in Russian).
- ³¹E. S. Mchedlova and D. I. Trubetskov, "Radiation from a stream of small interacting electron oscillators," *Tech. Phys. Lett.* **19**, 784–786 (1993).
- ³²E. S. Mchedlova and D. I. Trubetskov, "Characteristics of radiation in chains of coupled small volumes containing electron oscillators," *Tech. Phys.* **39**, 1061–1065 (1994).
- ³³L. A. Vainshtein and A. I. Kleev, "Cooperative radiation of the electron-oscillators," *Sov. Phys. Dokl.* **35**, 359–363 (1990).
- ³⁴N. S. Ginzburg and A. S. Sergeev, "Radiation instability in the layers of the excited oscillators," *Sov. J. Plasma Phys.* **17**, 762–768 (1991).